

FERMILAB-PUB-12-466-T, ANL-HEP-PR-12-58, EFI-12-20, MAN/HEP/2012/11
KCL-PH-TH/2012-30, LCTS/2012-15, CERN-PH-TH/2012-195, CNU-HEP-12-01

CPsuperH2.3: an Updated Tool for Phenomenology in the MSSM with Explicit CP Violation

J. S. Lee^{a,b}, M. Carena^c, J. Ellis^{d,e}, A. Pilaftsis^f and C. E. M. Wagner^{g,h}

^a Department of Physics, Chonnam National University,
300 Yongbong-dong, Buk-gu, Gwangju, 500-757, Republic of Korea

^b Department of Physics, National Tsing Hua University, Hsinchu, Taiwan 300

^c Fermilab, P.O. Box 500, Batavia IL 60510, U.S.A.

^d Theoretical Particle Physics and Cosmology Group, Department of Physics,
King's College London, London WC2R 2LS, United Kingdom

^e Theory Division, CERN, CH-1211 Geneva 23, Switzerland

^f Consortium for Fundamental Physics, School of Physics and Astronomy
University of Manchester, Manchester M13 9PL, United Kingdom

^g HEP Division, Argonne National Laboratory, 9700 Cass Ave., Argonne, IL 60439, USA

^h Enrico Fermi Institute, Univ. of Chicago, 5640 Ellis Ave., Chicago, IL 60637, USA

ABSTRACT

We describe the Fortran code **CPsuperH2.3**, which incorporates the following updates compared with its predecessor **CPsuperH2.0**. It implements improved calculations of the Higgs-boson masses and mixing including stau contributions and finite threshold effects on the tau-lepton Yukawa coupling. It incorporates the LEP limits on the processes $e^+e^- \rightarrow H_i Z, H_i H_j$ and the CMS limits on $H_i \rightarrow \bar{\tau}\tau$ obtained from 4.6 fb^{-1} of data at a centre-of-mass energy of 7 TeV. It also includes the decay mode $H_i \rightarrow Z\gamma$ and the Schiff-moment contributions to the electric dipole moments of Mercury and Radium 225, with several calculational options for the case of Mercury. These additions make **CPsuperH2.3** a suitable tool for analyzing possible CP-violating effects in the MSSM in the era of the LHC and a new generation of EDM experiments *.

PACS: 12.60.Jv, 13.20.He, 14.80.Cp

KEYWORDS: Higgs bosons; Supersymmetry; CP; LHC; EDMs.

*The program may be obtained from <http://www.hep.man.ac.uk/u/jslee/CPsuperH.html>, or by contacting the first author at jslee@jnu.ac.kr.

1 Introduction

Supersymmetry is one of the most attractive possible scenarios for physics beyond the Standard Model in the TeV energy range, and the minimal supersymmetric extension of the Standard Model (MSSM) is the simplest framework that incorporates this scenario. The MSSM allows for many possible CP-violating phases, notably those in the SU(3), SU(2) and U(1) gaugino masses $M_{3,2,1}$ and in the trilinear soft supersymmetry-breaking parameters associated with the third-generation Yukawa couplings $A_{t,b,\tau}$.

CPsuperH [1, 2] is an evolving software tool that incorporates the effects of these CP-violating phases into the calculation of Higgs boson masses, couplings and other properties. The previous version, **CPsuperH2.0** [1], also incorporated a number of B -physics observables, including the branching ratios for $B_s \rightarrow \mu^+ \mu^-$, $B_d \rightarrow \tau^+ \tau^-$, $B_u \rightarrow \tau \nu$, $B \rightarrow X_s \gamma$ and the CP-violating asymmetry in the latter decay, A_{CP} , as well as the supersymmetric contributions to the $B_{s,d}^0 - \bar{B}_{s,d}^0$ mass differences. Also included in **CPsuperH2.0** were calculations of two-loop supersymmetric Higgs contributions to the electric dipole moments (EDMs) of Thallium, the electron and muon [†].

After the recent discovery at the LHC [4] of a new particle resembling a Standard-Model-like Higgs boson, Higgs physics and searches for associated CP-violating effects are entering a new era, in which the LHC experiments are now also probing directly the possible existences of heavier supersymmetric Higgs bosons. In parallel, the LHCb experiment is taking experiments on B -physics to a new level of precision, and a new round of experiments is set to improve significantly sensitivities to a wider range of EDMs, including also Mercury and Radium. This juncture in the exploration of physics at the TeV scale, both direct and indirect, is the appropriate moment to document the capabilities of a new update of **CPsuperH**.

The followings are the main new features incorporated in **CPsuperH2.3**. As described in Section 2, it features an improved treatment of CP-violating effects on Higgs-boson masses and mixing, with stau contributions included as in Ref. [5]. We also take consistently into account finite radiative effects on the tau-lepton Yukawa coupling. As described in Section 3, **CPsuperH2.3** also features an implementation of the LEP limits on the processes $e^+ e^- \rightarrow H_i Z, H_i H_j$ [6], as well as the limits on $H_i \rightarrow \bar{\tau} \tau$ obtained by CMS with 4.6 fb^{-1} of LHC data at a centre-of-mass energy of 7 TeV [7], where H_i (with $i = 1, 2, 3$) denotes collectively the three neutral Higgs bosons $H_{1,2,3}$ in the CP-violating MSSM. In the same section, we also present theoretical predictions for $H_i \rightarrow Z \gamma$, as these decay modes can become detectable as the integrated LHC luminosity increases. Section 4 outlines how **CPsuperH2.3** incorporates calculations of the EDMs of Mercury and ^{225}Ra that include estimates of the contributions due to Schiff moments [8]. Each section includes figures that illustrate some typical results obtained using **CPsuperH2.3**. As explained in Section 5, an SLHA2 interface was created to facilitate the comparison and linkage of output data between **CPsuperH2.3** and other public codes, in accordance with the SUSY Les Houches Accord [10, 11]. Finally, Section 6 summarizes our updates to the code.

[†]For an alternative code treating similar physics, see [3].

2 Stau Contributions to Higgs masses and Mixing

The scalar tau contributions to the masses and mixing of the neutral Higgs bosons have been included as in Ref. [5], similarly to the sbottom corrections with

$$X_\tau = \frac{3g'^2 - g^2}{4} \frac{m_{\tilde{L}_3}^2 - m_{\tilde{E}_3}^2}{m_{\tilde{\tau}_2}^2 - m_{\tilde{\tau}_1}^2}. \quad (1)$$

More precisely, in the $(\phi_1, \phi_2, a)^T$ basis, the scalar tau contributions to the entries of the neutral Higgs mass squared matrix from the one-loop effective potential are given by

$$\begin{aligned} (\Delta \mathcal{M}_H^2)_{\phi_1 \phi_1}^{\tilde{\tau}} &= \frac{m_\tau^2}{8\pi^2} \left\{ |h_\tau|^2 \log \frac{m_{\tilde{\tau}_1}^2 m_{\tilde{\tau}_2}^2}{m_\tau^4} - \hat{g}^2 \log \frac{m_{\tilde{\tau}_1}^2 m_{\tilde{\tau}_2}^2}{Q_0^4} \right. \\ &\quad \left. + g(m_{\tilde{\tau}_1}^2, m_{\tilde{\tau}_2}^2) R'_\tau (|h_\tau|^2 R'_\tau + X_\tau) + \log \frac{m_{\tilde{\tau}_2}^2}{m_{\tilde{\tau}_1}^2} [X_\tau + (2|h_\tau|^2 - \hat{g}^2) R'_\tau] \right\}; \end{aligned} \quad (2)$$

$$\begin{aligned} (\Delta \mathcal{M}_H^2)_{\phi_1 \phi_2}^{\tilde{\tau}} &= \frac{m_\tau^2}{8\pi^2} \left\{ g(m_{\tilde{\tau}_1}^2, m_{\tilde{\tau}_2}^2) \left[|h_\tau|^2 R_\tau R'_\tau + \frac{X_\tau}{2} (R_\tau - R'_\tau \tan\beta) \right] + \frac{\hat{g}^2}{2} \tan\beta \log \frac{m_{\tilde{\tau}_1}^2 m_{\tilde{\tau}_2}^2}{Q_0^4} \right. \\ &\quad \left. + \log \frac{m_{\tilde{\tau}_2}^2}{m_{\tilde{\tau}_1}^2} \left[|h_\tau|^2 R_\tau - \frac{X_\tau}{2} \tan\beta + \frac{\hat{g}^2}{2} (R'_\tau \tan\beta - R_\tau) \right] \right\}; \end{aligned} \quad (3)$$

$$(\Delta \mathcal{M}_H^2)_{\phi_2 \phi_2}^{\tilde{\tau}} = \frac{m_\tau^2}{8\pi^2} \left[g(m_{\tilde{\tau}_1}^2, m_{\tilde{\tau}_2}^2) R_\tau (|h_\tau|^2 R_\tau - \tan\beta X_\tau) + \hat{g}^2 \tan\beta R_\tau \log \frac{m_{\tilde{\tau}_2}^2}{m_{\tilde{\tau}_1}^2} \right]; \quad (4)$$

$$(\Delta \mathcal{M}_H^2)_{a \phi_1}^{\tilde{\tau}} = \frac{1}{16\pi^2} \frac{m_\tau^2 \Delta_{\tilde{\tau}}}{\cos\beta} \left[-g(m_{\tilde{\tau}_1}^2, m_{\tilde{\tau}_2}^2) (X_\tau + 2|h_\tau|^2 R'_\tau) + (\hat{g}^2 - 2|h_\tau|^2) \log \frac{m_{\tilde{\tau}_2}^2}{m_{\tilde{\tau}_1}^2} \right]; \quad (5)$$

$$(\Delta \mathcal{M}_H^2)_{a \phi_2}^{\tilde{\tau}} = \frac{1}{16\pi^2} \frac{m_\tau^2 \Delta_{\tilde{\tau}}}{\cos\beta} \left[g(m_{\tilde{\tau}_1}^2, m_{\tilde{\tau}_2}^2) (X_\tau \tan\beta - 2|h_\tau|^2 R_\tau) - \hat{g}^2 \tan\beta \log \frac{m_{\tilde{\tau}_2}^2}{m_{\tilde{\tau}_1}^2} \right]; \quad (6)$$

where $\hat{g}^2 \equiv (g^2 + g'^2)/4$ and the CP-violating quantity is [‡]

$$\Delta_{\tilde{\tau}} \equiv -\frac{\Im m(A_\tau \mu)}{m_{\tilde{\tau}_2}^2 - m_{\tilde{\tau}_1}^2}. \quad (7)$$

The $\tan\beta$ -enhanced terms containing μ and A_τ are included in R_τ and R'_τ , given by

$$R_\tau = \frac{|A_\tau|^2 \tan\beta - \Re e(A_\tau \mu)}{m_{\tilde{\tau}_2}^2 - m_{\tilde{\tau}_1}^2}; \quad R'_\tau = \frac{|A_\tau|^2 - \Re e(A_\tau \mu) \tan\beta}{m_{\tilde{\tau}_2}^2 - m_{\tilde{\tau}_1}^2}, \quad (8)$$

and the loop function

$$g(m_1^2, m_2^2) \equiv 2 - \frac{m_1^2 + m_2^2}{m_1^2 - m_2^2} \log \frac{m_1^2}{m_2^2}. \quad (9)$$

[‡]To match the **CPsuperH** convention, the sign of A_τ is flipped compared to Ref. [5].

Since the stau contributions to the mass splitting $M_{H^\pm}^2 - M_A^2$ are small, we have neglected them. For the same reason, we set

$$\left(\Delta\mathcal{M}_H^2\right)_{aa}^{\tilde{\tau}} = 0. \quad (10)$$

Note that in the limit of small mass splitting one has

$$\frac{g(m_1^2, m_2^2)}{(m_2^2 - m_1^2)^2} \longrightarrow -\frac{1}{6M_S^2} \quad (11)$$

with $M_S^2 = (m_1^2 + m_2^2)/2$. So, in this limit, the leading contributions proportional to $\tan^4 \beta$ are given by

$$\begin{aligned} \left(\Delta\mathcal{M}_H^2\right)_{\phi_1\phi_1}^{\tilde{\tau}} &\approx -\frac{m_\tau^2}{48\pi^2} |h_\tau|^2 \frac{[\Re(A_\tau\mu)]^2}{M_S^4} \tan^2 \beta; \\ \left(\Delta\mathcal{M}_H^2\right)_{\phi_1\phi_2}^{\tilde{\tau}} &\approx +\frac{m_\tau^2}{48\pi^2} |h_\tau|^2 \frac{|\mu|^2 \Re(A_\tau\mu)}{M_S^4} \tan^2 \beta; \\ \left(\Delta\mathcal{M}_H^2\right)_{\phi_2\phi_2}^{\tilde{\tau}} &\approx -\frac{m_\tau^2}{48\pi^2} |h_\tau|^2 \frac{|\mu|^4}{M_S^4} \tan^2 \beta; \end{aligned} \quad (12)$$

which are the same as those presented in [12–14]. Note that here we take into account the $\tilde{\tau}_{1,2}$ mass splitting.

In Fig. 1, we demonstrate the impact of the corrections from the light scalar taus for large $\mu = 1$ TeV for several values of $\tan \beta$. When $m_{\tilde{\tau}_{1,2}} \sim 1$ TeV, the stau corrections are negligible and the lightest Higgs boson mass increases by the small amount of ~ 0.05 GeV even when $\tan \beta = 60$. However, these corrections are larger for lighter staus, and the lightest Higgs boson mass may decrease by as much as ~ 4 GeV, if $\tan \beta = 60$ and $m_{\tilde{\tau}_1} \sim 100$ GeV. For comparison, as shown in Table 4, the masses and mixing matrix of the neutral Higgs bosons without including the stau effects are stored in the array **RAUX_H**:

- **RAUX_H(511 – 513)** : Three Higgs masses without including the stau effects;
- **RAUX_H(520 – 528)** : The nine elements of the mixing matrix $O_{\alpha i}$ without including the stau effects.

3 Collider Limits

The limits on Higgs boson production at LEP and the LHC experiments have been implemented as follows.

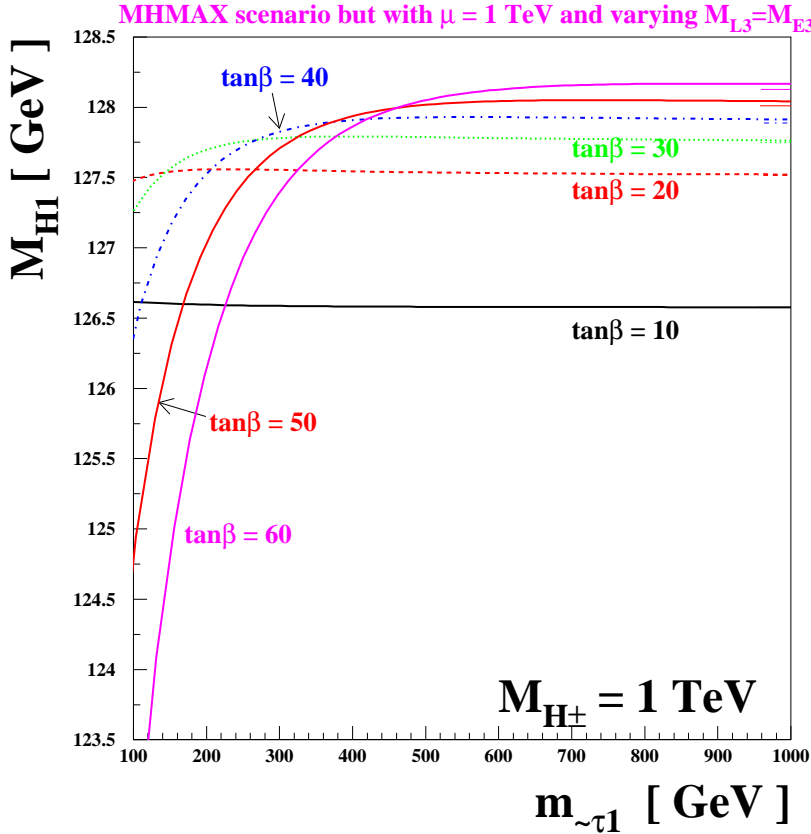


Figure 1: The lightest Higgs boson mass as a function of the lighter stau mass for several values of $\tan\beta$: $\tan\beta = 10$ (black), $\tan\beta = 20$ (red), $\tan\beta = 30$ (green), $\tan\beta = 40$ (blue), $\tan\beta = 50$ (yellow), and $\tan\beta = 60$ (magenta), as obtained varying $m_{\tilde{L}_3} = m_{\tilde{E}_3}$ with fixed $\mu = 1$ TeV. We use the MHMAX scenario for the other supersymmetric model parameters: $m_{\tilde{Q}_3} = m_{\tilde{U}_3} = m_{\tilde{D}_3} = M_{\text{SUSY}} = 1$ TeV, $M_1 = 100$ GeV, $M_2 = 200$ GeV, $M_3 = 800$ GeV, and $A_t = \sqrt{6} M_{\text{SUSY}} + \mu / \tan\beta$ with $A_b = A_\tau = A_t$. We have fixed $M_{H^\pm} = 1$ TeV. The thin short line around $m_{\tilde{\tau}_1} = 1$ TeV for each $\tan\beta$ value shows the lightest Higgs boson mass before the inclusion of the stau effects.

3.1 LEP Limits

We have implemented the LEP limits from the processes $e^+e^- \rightarrow H_iZ$ and $e^+e^- \rightarrow H_iH_j$ using Table 14(a) and Table 17(a) of Ref. [6], respectively, assuming that the Higgs decay patterns are not drastically different from those in the Standard Model and in the MHMAX scenario with $\tan\beta = 10$. We have required that each of the Higgs couplings to the gauge boson(s) normalized to the Standard Model values, $g_{H_iVV}^2$ and $g_{H_iH_jZ}^2$, should be smaller than the corresponding values in the Tables. The result is saved in

- RAUX_H(430)=ILEP : 0 (Excluded) or 1 (Allowed).

For the more general cases, we refer to more refined tools such as `HiggsBounds` [15].

3.2 LHC Limits

We have also incorporated the recent CMS limit from the search for the MSSM neutral Higgs bosons decaying into tau pairs based on 4.6 fb^{-1} [7], and the result is saved in

$$- \text{RAUX_H}(440) = \text{ILHC7}_{4.6}^{H \rightarrow \tau\tau} : 0 \text{ (Excluded) or } 1 \text{ (Allowed)} .$$

In our implementation of the CMS limit, assuming the same K factors as in the SM, we approximate the production cross sections of the neutral Higgs bosons at the LHC as follows:

$$\sigma_{\mathcal{P}}^{\text{MSSM}}(pp \rightarrow H_i X) \simeq \left(\frac{\Gamma_{\mathcal{P}}^{\text{MSSM}}}{\Gamma_{\mathcal{P}}^{\text{SM}}} \right)_i^{\text{LO}} \sigma_{\mathcal{P}}^{\text{SM}}(pp \rightarrow H_{\text{SM}} X) \Big|_{M_{H_{\text{SM}}} = M_{H_i}}, \quad (13)$$

where $\mathcal{P} = ggH_i, bbH_i, VVH_i$ specifies each production process. The SM production cross sections are calculated by using **HIGLU** [16], **BBHQNNLO** [17] and **HAWK** [18][§]. In leading order, the process-dependent ratios are given by:

- Gluon fusion

$$\left(\frac{\Gamma_{ggH_i}^{\text{MSSM}}}{\Gamma_{ggH_i}^{\text{SM}}} \right)_i^{\text{LO}} = \frac{|S_i^g(M_{H_i})|^2 + |P_i^g(M_{H_i})|^2}{|S_{\text{SM}}^g(M_{H_i})|^2} \equiv R_{H_igg}, \quad (14)$$

where $S_{\text{SM}}^g(M_{H_i}) = \sum_{f=b,t} F_{sf}(\tau_{if})$. These factors are saved in the array **CAUX_H(221–223)** as shown in Table 6.

- b -quark fusion

$$\left(\frac{\Gamma_{bbH_i}^{\text{MSSM}}}{\Gamma_{bbH_i}^{\text{SM}}} \right)_i^{\text{LO}} = |g_{H_i\bar{b}b}^S|^2 + \frac{|g_{H_i\bar{b}b}^P|^2}{(1 - 4m_b^2/M_{H_i}^2)} \equiv R_{H_i bb}. \quad (15)$$

where the extra factor in the second term accounts for the phase-space difference between scalar and pseudo-scalar decays.

- Vector-boson fusion

$$\left(\frac{\Gamma_{VVH_i}^{\text{MSSM}}}{\Gamma_{VVH_i}^{\text{SM}}} \right)_i^{\text{LO}} = g_{H_i VV}^2. \quad (16)$$

In Figs. 2,3,4, we show the three process-dependent ratios as functions of the corresponding Higgs masses, assuming the **MHMAX** scenario. For completeness, also shown in Fig. 5 are the ratios of the Higgs-boson couplings to two photons defined by

$$R_{H_i\gamma\gamma} \equiv \frac{|S_i^\gamma(M_{H_i})|^2 + |P_i^\gamma(M_{H_i})|^2}{|S_{\text{SM}}^\gamma(M_{H_i})|^2}, \quad (17)$$

[§]We thank Junya Nakamura for providing the SM cross sections.

MHMAX scenario

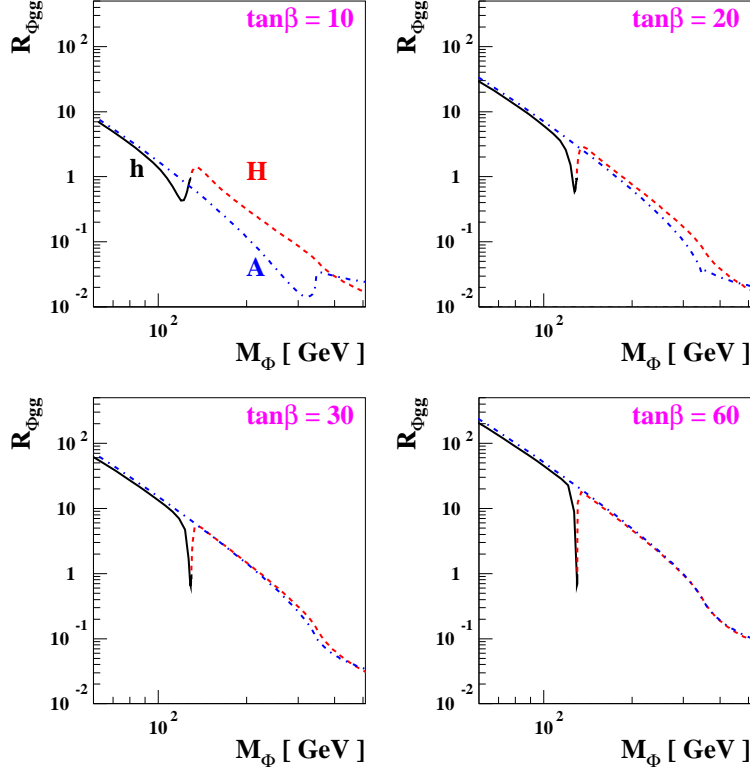


Figure 2: The couplings of the MSSM Higgs bosons Φ to two gluons normalized to the Standard Model values, $R_{H_1 gg}$ (14), as functions of their masses for several values of $\tan\beta$. In the CP-conserving limit, $\Phi \equiv h, H, A$ with $h(H)$ and A being the lighter (heavier) CP-even and CP-odd Higgs bosons, respectively. We assume the MHMAX scenario: $m_{\tilde{Q}_3} = m_{\tilde{U}_3} = m_{\tilde{D}_3} = m_{\tilde{L}_3} = m_{\tilde{E}_3} = M_{\text{SUSY}} = 1 \text{ TeV}$, $\mu = 200 \text{ GeV}$, $M_1 = 100 \text{ GeV}$, $M_2 = 200 \text{ GeV}$, $M_3 = 800 \text{ GeV}$, and $A_t = \sqrt{6} M_{\text{SUSY}} + \mu / \tan\beta$ with $A_b = A_\tau = A_t$.

where $S_{\text{SM}}^\gamma(M_{H_i}) \equiv 2 \sum_{f=b,t,c,\tau} N_C Q_f^2 F_{sf}(\tau_{if}) - F_{sf}(\tau_{iW})$, which are saved in the array CAUX_H(231–233) as shown in Table 6.

We observe that the branching ratio $B(H_1 \rightarrow \gamma\gamma)$ may be enhanced if the lighter stau has a low mass, particularly for large $\tan\beta$ as shown in Fig. 6. This enhancement is consistent with the signals observed [4], which may be larger than in the Standard Model. Furthermore, in Fig. 7 we show the correlation of $B(H_1 \rightarrow \gamma\gamma)$ with $B(H_1 \rightarrow Z\gamma)$ in the MSSM, after the branching ratios are normalized to their SM predictions. Calculational details of $B(H_i \rightarrow Z\gamma)$ are described in Appendix A.

MHMAX scenario

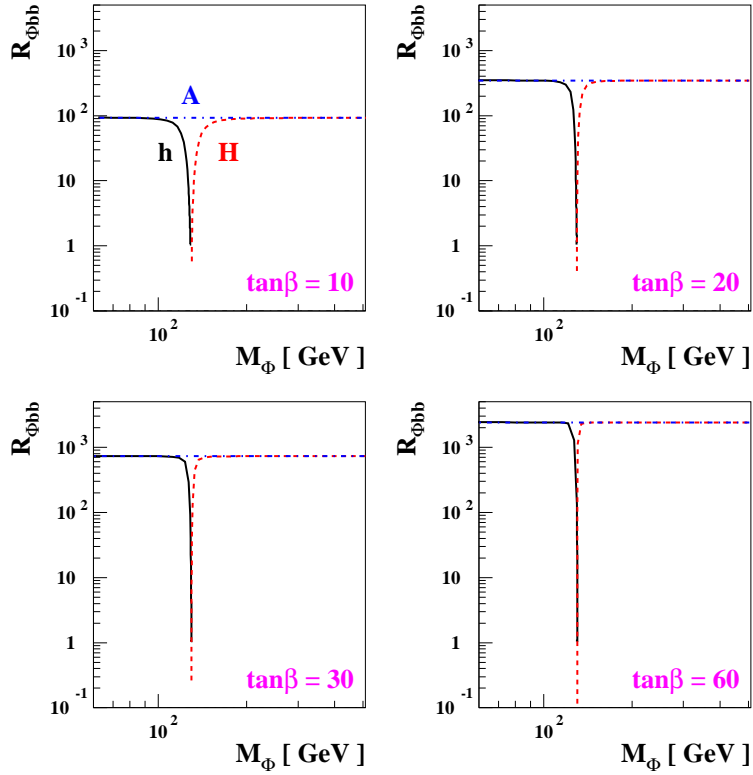


Figure 3: The same as in Fig. 2 but for the couplings of the Higgs bosons to b quarks (15).

Once the production cross sections of the neutral MSSM Higgs bosons have been calculated, we may require the sum ¶

$$\sigma(pp \rightarrow H_i X) \cdot B(H_i \rightarrow \tau\tau) + \sum_{\phi \neq H_i} \left|_{|M_\phi - M_{H_i}| \leq \delta M} \right. \sigma(pp \rightarrow \phi X) \cdot B(\phi \rightarrow \tau\tau) \quad (18)$$

to be smaller than the observed limit for a given value M_{H_i} of a specified neutral Higgs boson H_i . Here we are adding all Higgs production cross sections of $\phi \neq H_i$ to the one of the H_i boson when their mass difference is smaller than δM . We take $\delta M = 0.21 * 130/2 \sim 13$ GeV, corresponding to the tau-pair mass resolution of $\sim 21\%$ at a Higgs boson mass of 130 GeV [7]. Such a simple treatment is fairly accurate, as long as $\delta M \gg \Gamma_{H_i}$, namely in the absence of strongly overlapping Higgs resonances [9]. Under these considerations, Fig. 8 shows the LEP- and LHC-excluded regions in the M_A - $\tan\beta$ plane for the MHMAX scenario. We find our results reasonably consistent with those presented in Fig. 4 of [7] when $M_A \geq 90$ GeV.

Finally, for the value given by $M_{H_{SM}} = \text{SMPARA_H}(20)$, the decay widths and branching ratios of the SM Higgs have been calculated, and the results are stored in $\text{RAUX_H}(600\text{-}700)$,

[¶]In the CP-conserving limit, the CP-odd state A is H_i with $O_{ai}^2 = 1$. In the CP-violating case, we identify the “CP-odd state” as the one which has the largest CP-odd component squared O_{ai}^2 .

MHMAX scenario

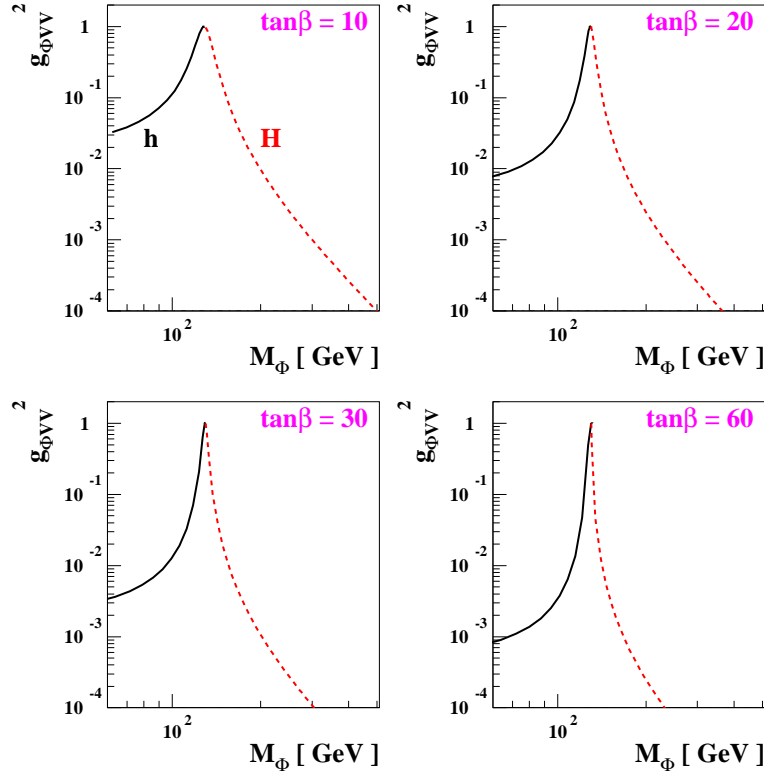


Figure 4: *The same as in Fig. 2 but for the couplings of the Higgs bosons to two vector bosons (16).*

see Table 4. For comparison with other works, we display in Fig. 9 the decay widths into b quarks and photons (upper) and the branching ratios into W and Z bosons (lower) as functions of the SM Higgs-boson mass. We note that decay widths into off-shell vector bosons using the four-body phase-space have been implemented in **CPsuperH2.3**.

4 Mercury and Radium Electric Dipole Moments

CPsuperH2.0 included two-loop Higgs-mediated contributions to the Thallium and electron EDMs [1], and **CPsuperH2.3** extends these results to include calculations of the Mercury and ^{225}Ra EDMs that incorporate Schiff-moment contributions. In the case of the Mercury EDM, these are parameterized as follows [19]:

$$\begin{aligned} d_{\text{Hg}}^{\text{I,II,III,IV}} &= d_{\text{Hg}}^{\text{I,II,III,IV}}[S] + 10^{-2}d_e^E + (3.5 \times 10^{-3}\text{GeV}) e C_S \\ &+ (4 \times 10^{-4} \text{ GeV}) e \left[C_P + \left(\frac{Z - N}{A} \right)_{\text{Hg}} C'_P \right], \end{aligned}$$

MHMAX scenario

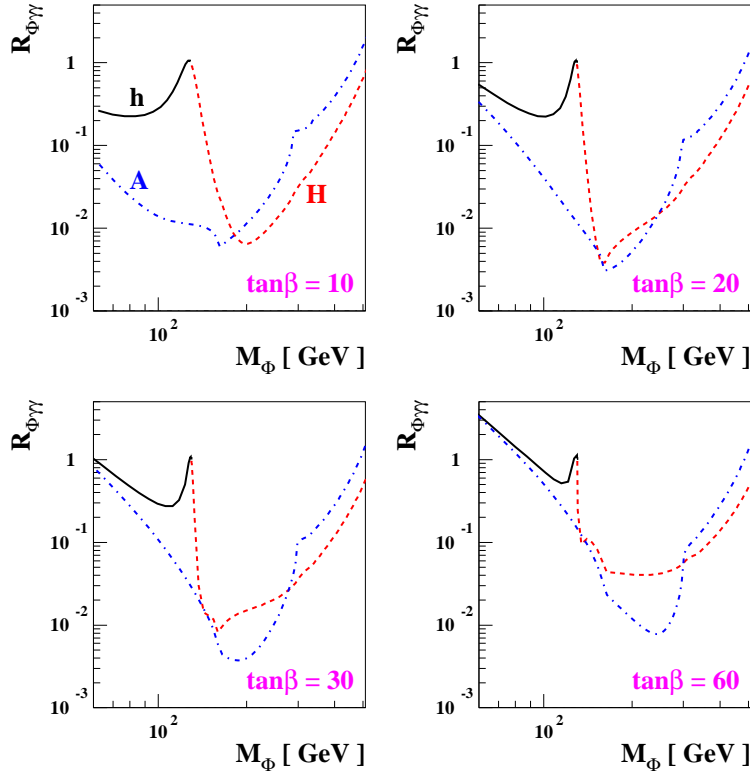


Figure 5: The same as in Fig. 2 but for the couplings of the Higgs bosons to two photons.

where $d_{\text{Hg}}^{\text{I,II,III,IV}}[S]$ denote the following four different Schiff-moment induced Mercury EDM calculations:

$$\begin{aligned} d_{\text{Hg}}^{\text{I}}[S] &\simeq 1.8 \times 10^{-3} e \bar{g}_{\pi NN}^{(1)} / \text{GeV}, \\ d_{\text{Hg}}^{\text{II}}[S] &\simeq 7.6 \times 10^{-6} e \bar{g}_{\pi NN}^{(0)} / \text{GeV} + 1.0 \times 10^{-3} e \bar{g}_{\pi NN}^{(1)} / \text{GeV}, \\ d_{\text{Hg}}^{\text{III}}[S] &\simeq 1.3 \times 10^{-4} e \bar{g}_{\pi NN}^{(0)} / \text{GeV} + 1.4 \times 10^{-3} e \bar{g}_{\pi NN}^{(1)} / \text{GeV}, \\ d_{\text{Hg}}^{\text{IV}}[S] &\simeq 3.1 \times 10^{-4} e \bar{g}_{\pi NN}^{(0)} / \text{GeV} + 9.5 \times 10^{-5} e \bar{g}_{\pi NN}^{(1)} / \text{GeV}, \end{aligned}$$

where the $\bar{g}_{\pi NN}^{(0),(1)}$ are the CP-odd πNN couplings, and we refer to Ref. [8] for further details. We note that d_{Hg}^{I} is basically the same as that calculated in **CPsuperH2.0**. In the case of the Radium ^{225}Ra , we estimate the EDM through [8]

$$d_{\text{Ra}} \simeq d_{\text{Ra}}[S] \simeq -8.7 \times 10^{-2} e \bar{g}_{\pi NN}^{(0)} / \text{GeV} + 3.5 \times 10^{-1} e \bar{g}_{\pi NN}^{(1)} / \text{GeV}. \quad (19)$$

Fig. 10 shows the four estimates of the Mercury EDM and the Radium EDM as functions of the parameter ρ that parameterizes the hierarchy between the first two and third generations in the **CPX** scenario. The new EDMs are stored in the array **RAUX_H**:

- $\text{RAUX_H}(411) = d_{\text{Hg}}^{\text{I}}$, $\text{RAUX_H}(412) = d_{\text{Hg}}^{\text{II}}$, $\text{RAUX_H}(413) = d_{\text{Hg}}^{\text{III}}$, $\text{RAUX_H}(414) = d_{\text{Hg}}^{\text{IV}}$

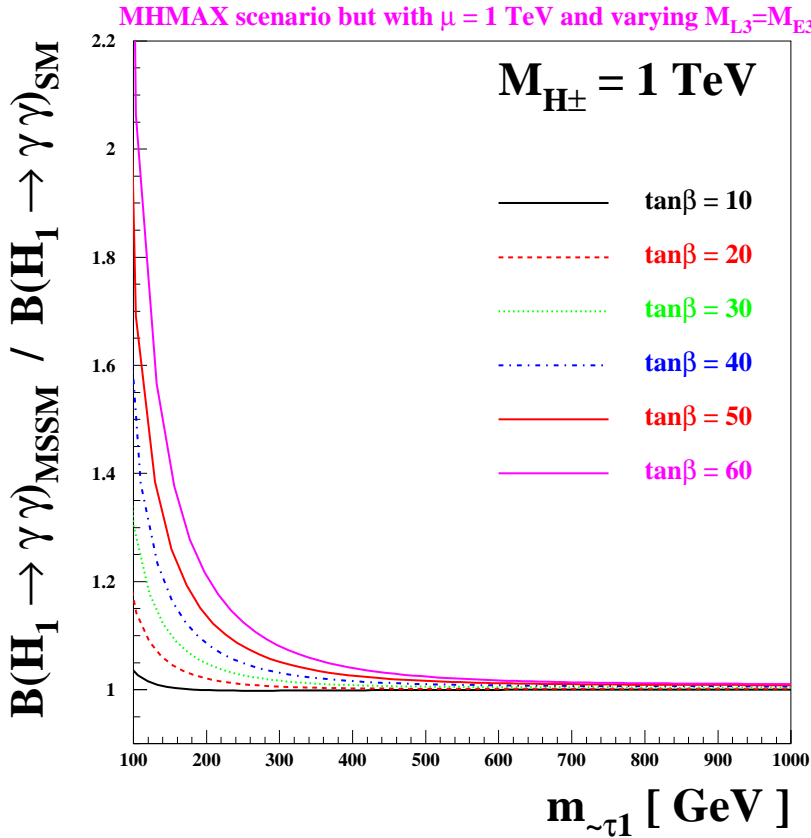


Figure 6: The ratio of the MSSM-to-SM branching ratios of the lightest Higgs boson H_1 decaying into photons as a function of the lighter stau mass. The scenario and lines are the same as in Fig. 1.

- RAUX_H(420) = d_{Ra}

as shown in Table 3.

5 SLHA2 interface ^{||}

CPsuperH2.3 also provides an output in accordance with the SUSY Les Houches Accords 1 (SLHA1) [10] and 2 (SLHA2) [11]. By taking **

- IFLAG_H(30)=1

in the run file, the output file cpsuper2.3_slha2.out is generated. The output file of the current version includes the following blocks:

^{||}We thank Alexander Pukhov for helpful discussions regarding the interface.

**Note that the default setting is IFLAG_H(30)=0, which is not recommended for generating files when a scan of the parameter space is performed.

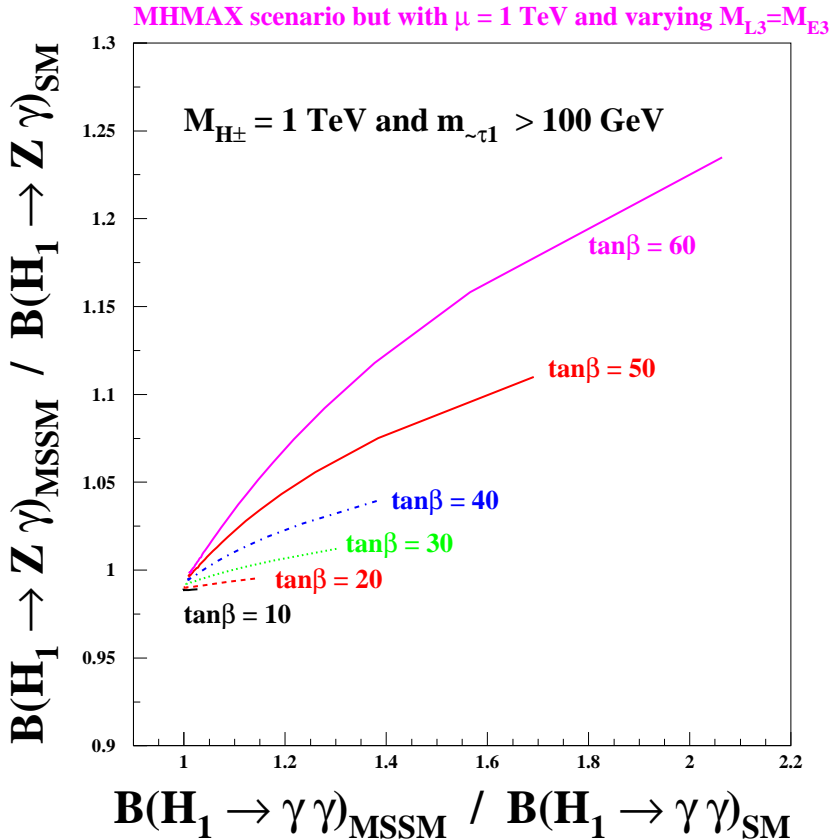


Figure 7: Correlations of the MSSM-to-SM branching ratio of the lightest Higgs boson H_1 decaying into two photons with the respective one for the decay H_1 into a Z boson and a photon, for discrete choices of $\tan\beta$. The scenario and lines are the same as in Fig. 1.

- **MODSEL:** In the block **MODSEL**, CP violation with completely general CP phases has been selected.
- **SMINPUTS** and **VCKMIN:** The quantities $\alpha_{\text{em}}^{-1}(M_Z)^{\overline{\text{MS}}}$, G_F , $\alpha_s(M_Z)^{\overline{\text{MS}}}$, M_Z , $m_b(m_b)^{\overline{\text{MS}}}$, $m_c(m_c)^{\overline{\text{MS}}}$, pole masses of top-quark, electron and muon, and $m_{d,u,s}(2 \text{ GeV})^{\overline{\text{MS}}}$ are given in the **SMINPUTS** block. In the **VCKMIN** block, the four parameters for the CKM mixing matrix λ , A , $\bar{\rho}$, and $\bar{\eta}$ are given.
- **EXTPAR** and **IMEXTPAR:** The blocks for non-minimal parameters have been filled according to Section 2 of the SLHA2 writeup [11] ††. For the input scale M_{input} , we are taking Q_{tb} , the scale of the heaviest third-generation squark [20], which is stored in **RAUX_H(13)=Q_{tb}²**. The imaginary parts of the gaugino masses, the trilinear couplings, and the μ parameters are listed in the block **IMEXTPAR**.
- **MASS:** In the **MASS** block, the pole masses of the neutral and charged Higgs bosons are given, and the W -boson mass is calculated from the Fermi constant via $M_W =$

††For the Higgs parameters, only the relevant quantities $\mu(M_{\text{input}})$, $\tan\beta(M_{\text{input}})$, and the charged Higgs pole mass have been included.

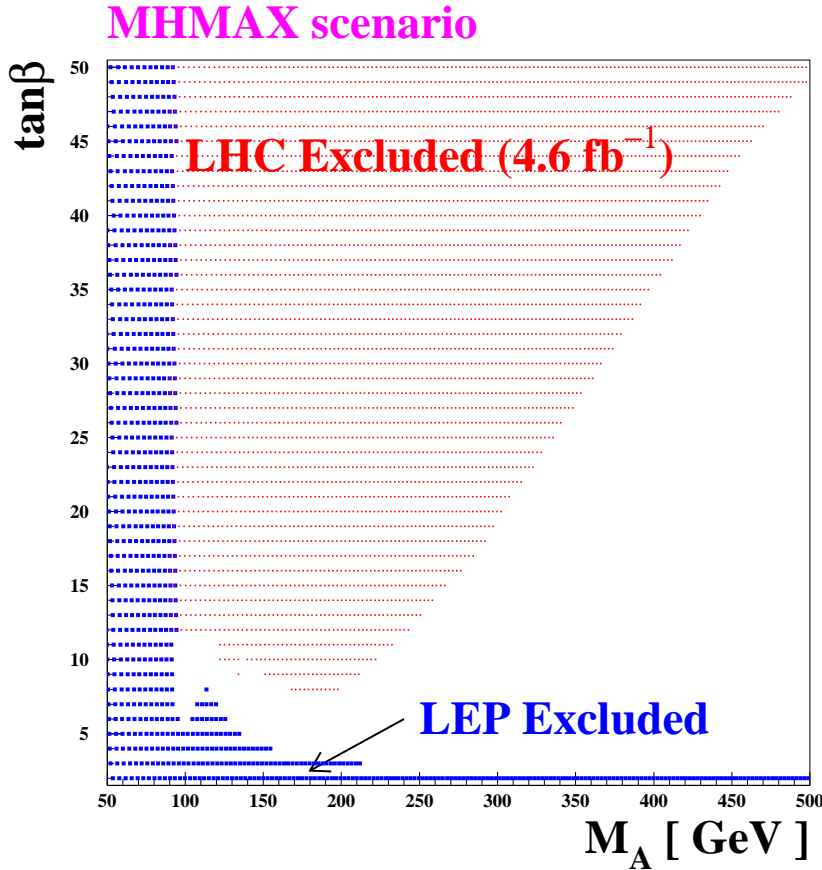


Figure 8: The LEP and LHC exclusion regions in the MHMAX scenario.

$\left(g^2/4\sqrt{2}G_F\right)^{1/2}$. Note that, in the present version, the tree-level masses of the third-generation sfermions, neutralinos, and charginos are given.

- **HCOUPLINGS, IMHCOUPLINGS:** In these blocks, the seven Higgs-self couplings λ_{1-7} calculated according to Ref. [21] are given from **CAUX_H(201–207)**.
- **THRESHOLD:** In this block, the measures of the threshold corrections to the Yukawa couplings $h_{t,b}$ are given from **CAUX_H(211, 212)**. The quantity Δ_b is also available from **CAUX_H(10)**.
- **NMIX, IMNMIX; UMIX, IMUMIX; VMIX, IMVMIX; STOPMIX, IMSTOPMIX; SBOTMIX, IMSBOTMIX; STAUMIX, IMSTAUMIX:** In these blocks, the mixing matrices of neutralinos, charginos, sfermions are given. Precisely,

- $(NMIX + I IMNMIX)_{i\alpha} = N_{i\alpha}$ with $i = 1, 2, 3, 4$ and $\alpha = (\tilde{B}, \tilde{W}^3, \tilde{H}_1^0, \tilde{H}_2^0)$,
- $(UMIX + I IMUMIX)_{i\alpha} = (C_L)_{i\alpha}$ with $i = 1, 2$ and $\alpha = (\tilde{W}^-, \tilde{H}^-)_L$,
- $(VMIX + I IMVMIX)_{i\alpha} = (C_R)_{i\alpha}^*$ with $i = 1, 2$ and $\alpha = (\tilde{W}^-, \tilde{H}^-)_R$,
- $(STOPMIX + I IMSTOPMIX)_{i\alpha} = (U^{\tilde{t}})_{\alpha i}^*$ with $i = 1, 2$ and $\alpha = (\tilde{t}_L, \tilde{t}_R)$, and similarly for sbottoms and staus.

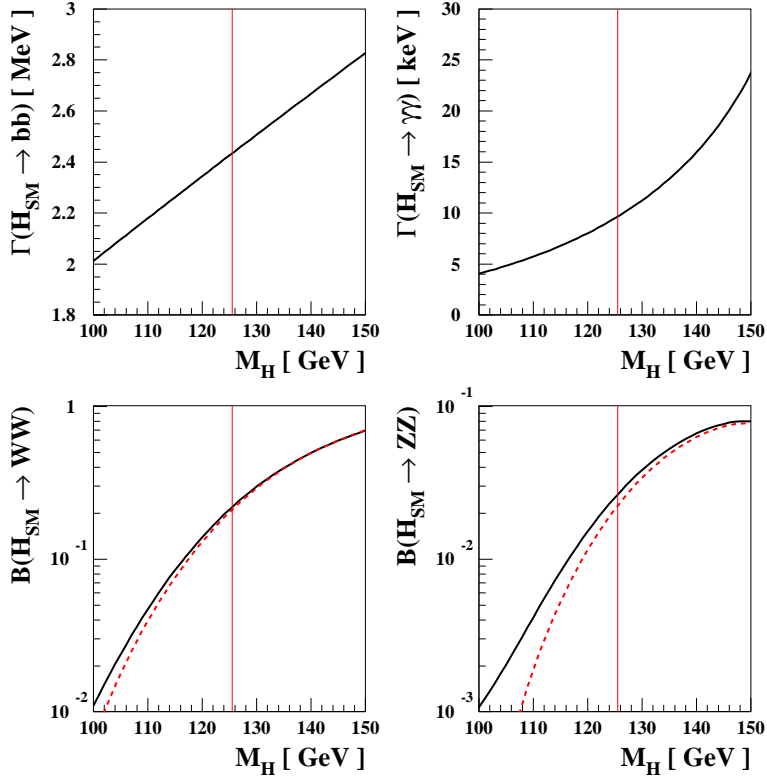


Figure 9: The upper frames are for the decay widths of the SM Higgs boson into b quarks (upper left) and photons (upper right) as functions of its mass. The lower frames are for the branching ratios into W (lower left) and Z (lower right) bosons. In the lower frames, the solid (dotted) lines are obtained using 4 (3)-body phase space below the mass thresholds. The vertical lines correspond to $M_{H_{\text{SM}}} = 125.5 \text{ GeV}$.

- CVHMIX: The block for the neutral Higgs boson mixing has been filled as suggested in Ref. [11]:

$$(\text{CVHMIX})_{i\sigma} = \begin{pmatrix} & 0 \\ O_{3 \times 3}^T & 0 \\ & 0 \end{pmatrix}_{i\alpha} \begin{pmatrix} 1 & 0 & 0 & 0 \\ 0 & 1 & 0 & 0 \\ 0 & 0 & -\sin \beta & \cos \beta \\ 0 & 0 & \cos \beta & \sin \beta \end{pmatrix}_{\alpha\sigma}, \quad (20)$$

with $i = 1, 2, 3$, $\alpha = (\phi_1, \phi_2, a, G^0)$ and $\sigma = (\phi_1, \phi_2, a_1, a_2)$. We note that $a = -\sin \beta a_1 + \cos \beta a_2$ and $G^0 = \cos \beta a_1 + \sin \beta a_2$.

- AU, IMAU, AD, IMAD, AE, IMAE; YU, IMYU, YD, IMYD, YE, IMYE: In these blocks, the third-generation (3, 3) components of the trilinear-coupling and the Yukawa-coupling matrices are given at the scales Q_{tb} and m_t^{pole} , respectively.
- DECAY: The total decay widths and the non-vanishing branching ratios of the neutral and charged Higgs bosons are stored in the block from the arrays `GAMBRN(101, 1, IH)`

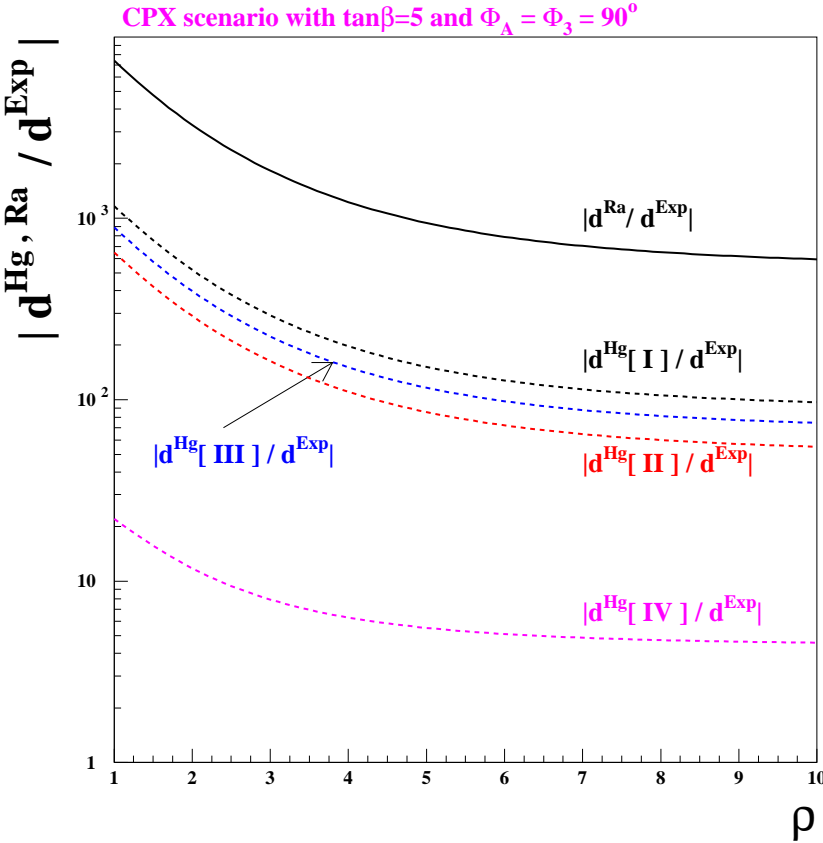


Figure 10: The four Mercury EDMs and the Radium EDM as functions of the parameters ρ that parameterizes the hierarchy between the first two and third generations as $m_{\tilde{X}_{1,2}} = \rho m_{\tilde{X}_3}$ with $X = Q, U, D, L, E$. The CPX scenario has been taken with $\tan \beta = 5$, $\Phi_{A_{t,b}} = \Phi_3 = 90^\circ$, and $M_{\text{SUSY}} = 0.5$ TeV: $m_{\tilde{Q}_3} = m_{\tilde{U}_3} = m_{\tilde{D}_3} = m_{\tilde{L}_3} = m_{\tilde{E}_3} = M_{\text{SUSY}}$; $|\mu| = 4 M_{\text{SUSY}}$, $|A_{t,b,\tau}| = 2 M_{\text{SUSY}}$, $|M_3| = 1$ TeV; $M_2 = 2M_1 = 100$ GeV, $M_{H^\pm} = 300$ GeV.

and GAMBRN(IM,3,IH) with IH= 1–3 and GAMBRC(51,1) and GAMBRC(IM,3), respectively. The decay width and branching ratios of the top quark are also stored from the arrays RAUX_H(50–53).

- **FOBS:** In this block, we show the branching ratios $B(b \rightarrow X_s \gamma)$, $B(B_s \rightarrow \mu\mu)$, $B(B_d \rightarrow \tau\tau)$, the ratio $R_{B\tau\nu}$, and the CP asymmetry $\mathcal{A}_{\text{CP}}(B \rightarrow X_s \gamma)$. These quantities are also available from RAUX_H(130,131) and RAUX_H(134,135,136) in different normalizations.
- **FOBSBSM:** In this block, we show the SUSY contributions to $\Delta M_{B_d, B_s}$ from RAUX_H(132,133). For the total $\Delta M_{B_d, B_s}$, one may add the quantities $\langle \bar{B}_d^0 | H_{\text{eff}}^{\Delta B=2} | B_d^0 \rangle_{\text{SUSY}}$ and $\langle \bar{B}_s^0 | H_{\text{eff}}^{\Delta B=2} | B_s^0 \rangle_{\text{SUSY}}$ given in CAUX_H(150,151) to the SM contributions.
- **FIDIPOLE:** Here, we list the EDMs of Thallium, neutron, Mercury, Deuteron, Radium, and muon, as well as the anomalous magnetic moment of muon, $(g_\mu - 2)$. In the cases of the neutron and Mercury EDMs, we present 3 and 4 evaluations, respectively, for

the estimation of the theoretical uncertainties.

- **HiggsBoundsInputHiggsCouplingsBosons**, **HiggsBoundsInputHiggsCouplingsFermions**: In these blocks, the Higgs couplings normalized to the corresponding SM couplings are listed for the interface to the program **HiggsBounds** [15].

6 Summary

Encouraged by the recent observation of a new particle resembling a SM-like Higgs boson at the CERN Large Hadron Collider [4], in **CPsuperH2.3** we have performed a number of updates to the **CPsuperH** code. In detail, we have improved the computation of CP-violating effects on Higgs-boson masses and mixing, by including stau contributions [5] and finite radiative effects on the tau-lepton Yukawa coupling. These effects play an important role in the decays $H_{1,2,3} \rightarrow \gamma\gamma$, for large values of $\tan\beta$ [14, 22]. We have also implemented the LEP limits on the processes $e^+e^- \rightarrow H_i Z, H_i H_j$, including the bounds on $H_i \rightarrow \bar{\tau}\tau$ obtained by CMS with 4.6 fb^{-1} of LHC data at a centre-of-mass energy of 7 TeV. Finally, we have included the decay modes of the neutral Higgs bosons $H_{1,2,3}$ into a Z boson and a photon. These decay modes are expected to become observable as more luminosity is accumulated at the LHC.

We have also incorporated in **CPsuperH2.3** calculations of the EDMs of Mercury and ^{225}Ra , including estimates of the contributions due to Schiff moments. We have presented a number of numerical examples and figures for each of our updates, in order to illustrate some typical results obtained by **CPsuperH2.3**. To enhance the synergy and compatibility of **CPsuperH2.3** with other codes, we have created an SLHA2 interface in accordance with the SUSY Les Houches Accords. For comparison with other works, we include evaluations of the principal decay rates and branching ratios of a SM Higgs boson. In the Appendix, we exhibit a number of output Tables, in order to highlight the updates with respect to the older version of **CPsuperH**.

If indeed the new particle discovered by ATLAS and CMS turns out to be a Higgs boson, the joint task of theory and experiment will be to establish whether it is compatible with the SM or exhibits deviations characteristic of some extension of the SM such as the MSSM. The possibility of CP violation should be considered in studying the latter possibility, and **CPsuperH2.3** is a suitable updated tool for this task.

Acknowledgements

We thank Genevieve Belanger, Kaoru Hagiwara, Sabine Kraml, Junya Nakamura and Alexander Pukhov for helpful discussions. The work of JSL is supported in part by the NSC of Taiwan (100-2112-M-007-023-MY3), the work of JE by the London Centre for Terauniverse Studies (LCTS), using funding from the European Research Council via the Advanced Investigator Grant 267352, and the work of AP by the Lancaster–Manchester–Sheffield Consortium for Fundamental Physics, under STFC research grant ST/J000418/1.

Fermilab is operated by Fermi Research Alliance, LLC under Contract No. DE-AC02-07CH11359 with the U.S. Department of Energy. Work at ANL is supported in part by the U.S. Department of Energy under Contract No. DE-AC02-06CH11357.

Appendix

Most importantly, in addition to the **SLHA2** interface, the array for the SM parameters **SMPARA_H** has been extended to include the SM Higgs mass, $M_{H_{\text{SM}}}$, see Table 1. Because of these improvements, from **CPsuperH2.2** to **CPsuperH2.3**, the following changes to the files **run** and **cpsuperh2.f** are needed:

- In the **run** file: the entries **SMPARA_H(20)** and **IFLAG_H(30)** added
- In the **cpsuperh2.f** file:
 - **REAL*8 SMPARA_H(19),SSPARA_H(38) \Rightarrow REAL*8 SMPARA_H(20),SSPARA_H(38)**
 - **DATA NSMIN/19/ \Rightarrow DATA NSMIN/20/**

Furthermore, in the updated version, the contents of the array **GAMBRN(IM,IWB=2,IH)** for the neutral Higgs-boson decays now include the corresponding SM branching ratios. To reproduce Figs. 6 and 7, for example, one simply needs to use the following ratios of parameter arrays:

$$\frac{B(H_1 \rightarrow \gamma\gamma)_{\text{MSSM}}}{B(H_1 \rightarrow \gamma\gamma)_{\text{SM}}} = \frac{\text{GAMBRN}(IM = 17, IWB = 3, IH = 1)}{\text{GAMBRN}(IM = 17, IWB = 2, IH = 1)};$$

$$\frac{B(H_1 \rightarrow Z\gamma)_{\text{MSSM}}}{B(H_1 \rightarrow Z\gamma)_{\text{SM}}} = \frac{\text{GAMBRN}(IM = 19, IWB = 3, IH = 1)}{\text{GAMBRN}(IM = 19, IWB = 2, IH = 1)}.$$

A $H_i \rightarrow Z\gamma$

For the calculation of $B(H_i \rightarrow Z\gamma)$, we closely follow Ref. [27].

The amplitude for the decay process $H_i \rightarrow Z(k_1, \epsilon_1) \gamma(k_2, \epsilon_2)$ can be written as

$$\mathcal{M}_{Z\gamma H_i} = -\frac{\alpha}{2\pi v} \left\{ S_i^{Z\gamma}(M_{H_i}) [k_1 \cdot k_2 \epsilon_1^* \cdot \epsilon_2^* - k_1 \cdot \epsilon_2^* k_2 \cdot \epsilon_1^*] - P_i^{Z\gamma}(M_{H_i}) \langle \epsilon_1^* \epsilon_2^* k_1 k_2 \rangle \right\} \quad (\text{A.1})$$

where $k_{1,2}$ are the momenta of the Z boson and the photon (we note that $2k_1 \cdot k_2 = M_{H_i}^2 - M_Z^2$), $\epsilon_{1,2}$ are their polarization vectors, and $\langle \epsilon_1^* \epsilon_2^* k_1 k_2 \rangle \equiv \epsilon_{\mu\nu\alpha\beta} \epsilon_1^\mu \epsilon_2^\nu k_1^\alpha k_2^\beta$. The decay width is given by

$$\begin{aligned} \Gamma(H_i \rightarrow Z\gamma) &= \frac{\alpha G_F^2 M_W^2 s_W^2}{64\pi^4} M_{H_i}^3 \left(1 - \frac{M_Z^2}{M_{H_i}^2}\right)^3 \left(\left|F_i^{(0)}(M_{H_i})\right|^2 + \left|F_i^{(5)}(M_{H_i})\right|^2\right) \\ &= \frac{\alpha^2 M_{H_i}^3}{128\pi^3 v^2} \left(1 - \frac{M_Z^2}{M_{H_i}^2}\right)^3 \left(\left|F_i^{(0)}(M_{H_i})\right|^2 + \left|F_i^{(5)}(M_{H_i})\right|^2\right). \end{aligned} \quad (\text{A.2})$$

The scalar and pseudoscalar form factors are given by

$$\begin{aligned} S_i^{Z\gamma}(M_{H_i}) &= \sum_{f=t,b,\tau} A_f^{(0)} + A_{\tilde{\chi}^\pm}^{(0)} + A_W + A_{H^\pm} + \sum_{f=t,b,\tau} A_{\tilde{f}}, \\ P_i^{Z\gamma}(M_{H_i}) &= \sum_{f=t,b,\tau} A_f^{(5)} + A_{\tilde{\chi}^\pm}^{(5)}, \end{aligned} \quad (\text{A.3})$$

with

$$\begin{aligned} A_f^{(0),(5)} &= 2Q_f N_C^f m_f^2 \frac{I_3^f - 2s_W^2 Q_f^2}{s_W c_W} g_{H_i \tilde{f} f}^{S,P} F_f^{(0),(5)}, \\ A_{\tilde{\chi}^\pm}^{(0),(5)} &= -M_Z^2 \cot \theta_W F_{\tilde{\chi}^\pm}^{(0),(5)}, \\ A_W &= M_Z^2 \cot \theta_W g_{H_i VV} F_W, \\ A_{H^\pm} &= -\frac{v^2}{2c_W s_W} g_{H_i H^+ H^-} F_{H^\pm}, \\ A_{\tilde{f}} &= M_Z^2 N_C^f Q_f F_{\tilde{f}}. \end{aligned} \quad (\text{A.4})$$

The loop functions are ^{††}

$$\begin{aligned} F_f^{(0)} &= C_0(m_f^2) + 4C_2(m_f^2), \\ F_f^{(5)} &= C_0(m_f^2), \\ F_{\tilde{\chi}^\pm}^{(0)} &= 2\sqrt{2} \sum_{j,k} \frac{m_{\tilde{\chi}_j^\pm}}{M_W} f \left(m_{\tilde{\chi}_j^\pm}, m_{\tilde{\chi}_k^\pm}, m_{\tilde{\chi}_k^\pm} \right) v_{Z\tilde{\chi}_j^\pm \tilde{\chi}_k^\pm} g_{H_i \tilde{\chi}_k^\pm \tilde{\chi}_j^\pm}^S, \\ F_{\tilde{\chi}^\pm}^{(5)} &= 2\sqrt{2} i \sum_{j,k} \frac{m_{\tilde{\chi}_j^\pm}}{M_W} g \left(m_{\tilde{\chi}_j^\pm}, m_{\tilde{\chi}_k^\pm}, m_{\tilde{\chi}_k^\pm} \right) v_{Z\tilde{\chi}_j^\pm \tilde{\chi}_k^\pm} g_{H_i \tilde{\chi}_k^\pm \tilde{\chi}_j^\pm}^P, \\ F_W &= 2 \left[\frac{M_{H_i}^2}{M_W^2} (1 - 2c_W^2) + 2(1 - 6c_W^2) \right] C_2(M_W^2) + 4(1 - 4c_W^2) C_0(M_W^2), \\ F_{H^\pm} &= 4C_2(M_{H^\pm}^2), \\ F_{\tilde{f}} &= -\frac{4v^2}{M_Z^2 c_W s_W} \sum_{j,k} g_{H_i \tilde{f}_j^* \tilde{f}_k} g_{Z \tilde{f}_k^* \tilde{f}_j} C_2(m_{\tilde{f}_j}, m_{\tilde{f}_k}, m_{\tilde{f}_k}). \end{aligned} \quad (\text{A.5})$$

We follow the conventions and notations of **CPsuperH** [2] for the Higgs couplings to the SM and supersymmetric particles, and the relevant Z -boson interactions are given by the following Lagrangian terms:

- Z -sfermion-sfermion

$$\mathcal{L}_{Z\tilde{f}\tilde{f}} = -ig_Z g_{Z\tilde{f}_j^* \tilde{f}_i} \left(\tilde{f}_j^* \overset{\leftrightarrow}{\partial}_\mu \tilde{f}_i \right) Z^\mu, \quad (\text{A.6})$$

where $g_Z = e/(s_W c_W)$ and

$$g_{Z\tilde{f}_j^* \tilde{f}_i} = I_3^f U_{Lj}^{\tilde{f}*} U_{Li}^{\tilde{f}} - Q_f s_W^2 \delta_{ij}. \quad (\text{A.7})$$

with $I_3^{u,\nu} = +1/2$ and $I_3^{d,e} = -1/2$.

^{††}For the functions of $C_{0,2}(m^2)$, $f(m_1, m_2, m_2)$, $g(m_1, m_2, m_2)$, and $C_2(m_1, m_2, m_2)$, we refer to [27].

- Z -chargino-chargino [28]

$$\mathcal{L}_{Z\tilde{\chi}^+\tilde{\chi}^-} = -g_Z \overline{\tilde{\chi}_i^-} \gamma^\mu \left(v_{Z\tilde{\chi}_i^+\tilde{\chi}_j^-} - a_{Z\tilde{\chi}_i^+\tilde{\chi}_j^-} \gamma_5 \right) \tilde{\chi}_j^- Z_\mu , \quad (\text{A.8})$$

where

$$\begin{aligned} v_{Z\tilde{\chi}_i^+\tilde{\chi}_j^-} &= \frac{1}{4} \left[(C_L)_{i2} (C_L)_{j2}^* + (C_R)_{i2} (C_R)_{j2}^* \right] - c_W^2 \delta_{ij} , \\ a_{Z\tilde{\chi}_i^+\tilde{\chi}_j^-} &= \frac{1}{4} \left[(C_L)_{i2} (C_L)_{j2}^* - (C_R)_{i2} (C_R)_{j2}^* \right] . \end{aligned} \quad (\text{A.9})$$

For completeness, we recall that the Z -boson couplings to the quarks and leptons are given by

$$\mathcal{L}_{Z\bar{f}f} = -g_Z \bar{f} \gamma^\mu \left(v_{Z\bar{f}f} - a_{Z\bar{f}f} \gamma_5 \right) f Z_\mu , \quad (\text{A.10})$$

with $v_{Z\bar{f}f} = I_3^f/2 - Q_f s_W^2$ and $a_{Z\bar{f}f} = I_3^f/2$.

B Tables updated

In this Appendix, we provide output Tables extended to include the updates implemented since the appearance of **CPsuperH2.0**.

Table 1: *The contents of the extended SMPARA_H(IP).*

IP	Parameter	IP	Parameter	IP	Parameter	IP	Parameter
1	$\alpha_{\text{em}}^{-1}(M_Z)$	6	m_μ	11	$m_u(m_t^{\text{pole}})$	16	λ
2	$\alpha_s(M_Z)$	7	m_τ	12	$m_c(m_t^{\text{pole}})$	17	A
3	M_Z	8	$m_d(m_t^{\text{pole}})$	13	m_t^{pole}	18	$\bar{\rho}$
4	$\sin^2 \theta_W$	9	$m_s(m_t^{\text{pole}})$	14	Γ_W	19	$\bar{\eta}$
5	m_e	10	$m_b(m_t^{\text{pole}})$	15	Γ_Z	20	$M_{H_{\text{SM}}}$

Table 2: *The contents of the extended SSPARA_H(IP).*

IP	Parameter	IP	Parameter	IP	Parameter	IP	Parameter
1	$\tan \beta$	11	$m_{\tilde{Q}_3}$	21	Φ_{A_τ}	31	$ A_u $
2	$M_{H^\pm}^{\text{pole}}$	12	$m_{\tilde{U}_3}$	22	$\rho_{\tilde{Q}}$	32	Φ_{A_u}
3	$ \mu $	13	$m_{\tilde{D}_3}$	23	$\rho_{\tilde{U}}$	33	$ A_c $
4	Φ_μ	14	$m_{\tilde{L}_3}$	24	$\rho_{\tilde{D}}$	34	Φ_{A_c}
5	$ M_1 $	15	$m_{\tilde{E}_3}$	25	$\rho_{\tilde{L}}$	35	$ A_d $
6	Φ_1	16	$ A_t $	26	$\rho_{\tilde{E}}$	36	Φ_{A_d}
7	$ M_2 $	17	Φ_{A_t}	27	$ A_e $	37	$ A_s $
8	Φ_2	18	$ A_b $	28	Φ_{A_e}	38	Φ_{A_s}
9	$ M_3 $	19	Φ_{A_b}	29	$ A_\mu $	39	...
10	Φ_3	20	$ A_\tau $	30	Φ_{A_μ}	40	...

Table 3: *The contents of the array RAUX_H. In RAUX_H(22) and RAUX_H(23), the notation h_f^0 is for the Yukawa couplings without including the threshold corrections. The notations are explained in Refs. [1, 2, 19, 20, 23–26]. For EDMs and the magnetic dipole moment (MDM) of the muon, some following slots of the array are allocated for the constituent contributions, see Refs. [19], [25] and [26] for details.*

RAUX_H(1)	m_b^{pole}	RAUX_H(130)	$B(B_s \rightarrow \mu\mu) \times 10^7$	RAUX_H(300)	$d_{\text{Tl}} e \text{ cm}$
RAUX_H(2)	$m_b(m_b^{\text{pole}})$	RAUX_H(131)	$B(B_d \rightarrow \tau\tau) \times 10^7$
RAUX_H(3)	$\alpha_s(m_b^{\text{pole}})$	RAUX_H(132)	$\Delta M_{B_d}^{\text{SUSY}} \text{ ps}^{-1}$	RAUX_H(310)	$d_n^{\text{CQM}} e \text{ cm}$
RAUX_H(4)	m_c^{pole}	RAUX_H(133)	$\Delta M_{B_s}^{\text{SUSY}} \text{ ps}^{-1}$
RAUX_H(5)	$m_c(m_c^{\text{pole}})$	RAUX_H(134)	$R_{B\tau\nu}$	RAUX_H(320)	$d_n^{\text{PQM}} e \text{ cm}$
RAUX_H(6)	$\alpha_s(m_c^{\text{pole}})$	RAUX_H(135)	$B(B \rightarrow X_s \gamma) \times 10^4$
...	...	RAUX_H(136)	$\mathcal{A}_{\text{CP}}(B \rightarrow X_s \gamma) \%$	RAUX_H(330)	$d_n^{\text{QCD}} e \text{ cm}$
...	...	RAUX_H(200)	$(d_e^E/e) \text{ cm}$	RAUX_H(340)	$d_{\text{Hg}} e \text{ cm}$
...
RAUX_H(10)	$M_{H^\pm}^{\text{pole}}$ or $M_{H^\pm}^{\text{eff.}}$	RAUX_H(210)	$(d_u^E/e) \text{ cm}$	RAUX_H(350)	$d_D e \text{ cm}$
RAUX_H(11)	Q_t^2
RAUX_H(12)	Q_b^2	RAUX_H(220)	$(d_d^E/e) \text{ cm}$	RAUX_H(360)	$(d_\mu/e) \text{ cm}$
RAUX_H(13)	Q_{tb}^2
RAUX_H(14)	$v_1(m_t^{\text{pole}})$	RAUX_H(230)	$(d_s^E/e) \text{ cm}$	RAUX_H(380)	$(a_\mu) \text{ SUSY}$
RAUX_H(15)	$v_1(Q_t)$
RAUX_H(16)	$v_1(Q_b)$	RAUX_H(240)	$d_u^C \text{ cm}$	RAUX_H(50)	$\Gamma(t \rightarrow W^+ b)$
RAUX_H(17)	$v_1(Q_{tb})$	RAUX_H(51)	$\Gamma(t \rightarrow H^+ b)$
RAUX_H(18)	$v_2(m_t^{\text{pole}})$	RAUX_H(250)	$d_d^C \text{ cm}$	RAUX_H(52)	$B(t \rightarrow W^+ b)$
RAUX_H(19)	$v_2(Q_t)$	RAUX_H(53)	$B(t \rightarrow H^+ b)$
RAUX_H(20)	$v_2(Q_b)$	RAUX_H(260)	$d^G \text{ cm/GeV}$
RAUX_H(21)	$v_2(Q_{tb})$	RAUX_H(400)	$d_s^C \text{ cm}$
RAUX_H(22)	$ h_t^0(m_t^{\text{pole}}) $	RAUX_H(270)	$C_S \text{ cm/GeV}$
RAUX_H(23)	$ h_b^0(m_t^{\text{pole}}) $	RAUX_H(271)	$C_P \text{ cm/GeV}$	RAUX_H(410)	$d_{\text{Hg}} e \text{ cm}$
RAUX_H(24)	$ h_t(m_t^{\text{pole}}) $	RAUX_H(272)	$C'_P \text{ cm/GeV}$	RAUX_H(411)	$d_{\text{Hg}}^I e \text{ cm}$
RAUX_H(25)	$ h_t(Q_t) $	RAUX_H(412)	$d_{\text{Hg}}^{II} e \text{ cm}$
RAUX_H(26)	$ h_t(Q_{tb}) $	RAUX_H(280)	$C_{de}/m_d \text{ cm/GeV}^2$	RAUX_H(413)	$d_{\text{Hg}}^{III} e \text{ cm}$
RAUX_H(27)	$ h_b(m_t^{\text{pole}}) $	RAUX_H(281)	$C_{se}/m_s \text{ cm/GeV}^2$	RAUX_H(414)	$d_{\text{Hg}}^{IV} e \text{ cm}$
RAUX_H(28)	$ h_b(Q_b) $	RAUX_H(282)	$C_{ed}/m_d \text{ cm/GeV}^2$
RAUX_H(29)	$ h_b(Q_{tb}) $	RAUX_H(283)	$C_{es}/m_s \text{ cm/GeV}^2$	RAUX_H(420)	$d_{\text{Ra}} e \text{ cm}$
RAUX_H(30)	M_A^2	RAUX_H(284)	$C_{eb}/m_b \text{ cm/GeV}^2$
RAUX_H(31)	$\Re e \hat{\Pi}_{H^+ H^-}(M_{H^\pm}^{\text{pole}})$	RAUX_H(285)	$C_{ec}/m_c \text{ cm/GeV}^2$	RAUX_H(430)	ILEP
RAUX_H(32)	$\bar{\lambda}_4 v^2(m_t^{\text{pole}})/2$	RAUX_H(286)	$C_{et}/m_t \text{ cm/GeV}^2$
RAUX_H(33)	$\bar{\lambda}_4(m_t^{\text{pole}})$	RAUX_H(287)	$C_{dd}/m_d \text{ cm/GeV}^2$	RAUX_H(440)	ILHC7 _{4.6} ^{H → ττ}
RAUX_H(34)	$\bar{\lambda}_1(m_t^{\text{pole}})$	RAUX_H(288)	$C_{sd}/m_s \text{ cm/GeV}^2$		
RAUX_H(35)	$\bar{\lambda}_2(m_t^{\text{pole}})$	RAUX_H(289)	$C_{bd}/m_b \text{ cm/GeV}^2$		
RAUX_H(36)	$\bar{\lambda}_{34}(m_t^{\text{pole}})$	RAUX_H(290)	$C_{db}/m_b \text{ cm/GeV}^2$		
...		
RAUX_H(101)	$\sqrt{\hat{s}}$		
...	22	...	

Table 4: *The contents of the array RAUX_H, continued.*

RAUX_H(501)	$m_b(M_{H_1})$	RAUX_H(600)	$M_{H_{\text{SM}}}$
RAUX_H(502)	$m_t(M_{H_1})$	RAUX_H(601)	$\Gamma(H_{\text{SM}} \rightarrow ee)$	RAUX_H(651)	$B(H_{\text{SM}} \rightarrow ee)$
RAUX_H(503)	$m_c(M_{H_1})$	RAUX_H(602)	$\Gamma(H_{\text{SM}} \rightarrow \mu\mu)$	RAUX_H(652)	$B(H_{\text{SM}} \rightarrow \mu\mu)$
RAUX_H(504)	$m_b(M_{H_2})$	RAUX_H(603)	$\Gamma(H_{\text{SM}} \rightarrow \tau\tau)$	RAUX_H(653)	$B(H_{\text{SM}} \rightarrow \tau\tau)$
RAUX_H(505)	$m_t(M_{H_2})$	RAUX_H(604)	$\Gamma(H_{\text{SM}} \rightarrow dd)$	RAUX_H(654)	$B(H_{\text{SM}} \rightarrow dd)$
RAUX_H(506)	$m_c(M_{H_2})$	RAUX_H(605)	$\Gamma(H_{\text{SM}} \rightarrow ss)$	RAUX_H(655)	$B(H_{\text{SM}} \rightarrow ss)$
RAUX_H(507)	$m_b(M_{H_3})$	RAUX_H(606)	$\Gamma(H_{\text{SM}} \rightarrow bb)$	RAUX_H(656)	$B(H_{\text{SM}} \rightarrow bb)$
RAUX_H(508)	$m_t(M_{H_3})$	RAUX_H(607)	$\Gamma(H_{\text{SM}} \rightarrow uu)$	RAUX_H(657)	$B(H_{\text{SM}} \rightarrow uu)$
RAUX_H(509)	$m_c(M_{H_3})$	RAUX_H(608)	$\Gamma(H_{\text{SM}} \rightarrow cc)$	RAUX_H(658)	$B(H_{\text{SM}} \rightarrow cc)$
...	...	RAUX_H(609)	$\Gamma(H_{\text{SM}} \rightarrow tt)$	RAUX_H(659)	$B(H_{\text{SM}} \rightarrow tt)$
RAUX_H(511)	$M_{H_1}(\tilde{f})$	RAUX_H(610)	$\Gamma(H_{\text{SM}} \rightarrow WW)$	RAUX_H(660)	$B(H_{\text{SM}} \rightarrow WW)$
RAUX_H(512)	$M_{H_2}(\tilde{f})$	RAUX_H(611)	$\Gamma(H_{\text{SM}} \rightarrow ZZ)$	RAUX_H(661)	$B(H_{\text{SM}} \rightarrow ZZ)$
RAUX_H(513)	$M_{H_3}(\tilde{f})$
...	...	RAUX_H(617)	$\Gamma(H_{\text{SM}} \rightarrow \gamma\gamma)$	RAUX_H(667)	$B(H_{\text{SM}} \rightarrow \gamma\gamma)$
RAUX_H(520)	$O_{\phi 1}(\tilde{f})$	RAUX_H(618)	$\Gamma(H_{\text{SM}} \rightarrow gg)$	RAUX_H(668)	$B(H_{\text{SM}} \rightarrow gg)$
RAUX_H(521)	$O_{\phi 2}(\tilde{f})$
RAUX_H(522)	$O_{\phi 3}(\tilde{f})$	RAUX_H(650)	$\Gamma_{\text{tot}}^{\text{SM}}$	RAUX_H(700)	$B_{\text{tot}}^{\text{SM}} = 1$
RAUX_H(523)	$O_{\phi 21}(\tilde{f})$
RAUX_H(524)	$O_{\phi 22}(\tilde{f})$
RAUX_H(525)	$O_{\phi 23}(\tilde{f})$
RAUX_H(526)	$O_{a 1}(\tilde{f})$
RAUX_H(527)	$O_{a 2}(\tilde{f})$
RAUX_H(528)	$O_{a 3}(\tilde{f})$
...

Table 5: The contents of the array CAUX_H. The notations are explained in Refs. [1, 2] and [24]. For CAUX_H(10,12), $h_q = h_q^0/(1 + \Delta_q \tan \beta)$.

CAUX_H(1)	$h_t/ h_t $	CAUX_H(130)	$S_1^\gamma(\sqrt{\hat{s}})$
CAUX_H(2)	$h_b/ h_b $	CAUX_H(131)	$P_1^\gamma(\sqrt{\hat{s}})$
CAUX_H(10)	Δ_b	CAUX_H(132)	$S_2^\gamma(\sqrt{\hat{s}})$
CAUX_H(11)	Δ_s	CAUX_H(133)	$P_2^\gamma(\sqrt{\hat{s}})$
CAUX_H(12)	$h_s(m_t^{\text{pole}})$	CAUX_H(134)	$S_3^\gamma(\sqrt{\hat{s}})$
CAUX_H(13)	h_τ	CAUX_H(135)	$P_3^\gamma(\sqrt{\hat{s}})$
...
CAUX_H(100)	$D_{1,1}^{H^0}(\hat{s})$
CAUX_H(101)	$D_{1,2}^{H^0}(\hat{s})$	CAUX_H(140)	$S_1^g(\sqrt{\hat{s}})$
CAUX_H(102)	$D_{1,3}^{H^0}(\hat{s})$	CAUX_H(141)	$P_1^g(\sqrt{\hat{s}})$
CAUX_H(103)	$D_{1,4}^{H^0}(\hat{s})$	CAUX_H(142)	$S_2^g(\sqrt{\hat{s}})$
CAUX_H(104)	$D_{2,1}^{H^0}(\hat{s})$	CAUX_H(143)	$P_2^g(\sqrt{\hat{s}})$
CAUX_H(105)	$D_{2,2}^{H^0}(\hat{s})$	CAUX_H(144)	$S_3^g(\sqrt{\hat{s}})$
CAUX_H(106)	$D_{2,3}^{H^0}(\hat{s})$	CAUX_H(145)	$P_3^g(\sqrt{\hat{s}})$
CAUX_H(107)	$D_{2,4}^{H^0}(\hat{s})$
CAUX_H(108)	$D_{3,1}^{H^0}(\hat{s})$	CAUX_H(150)	$\langle \bar{B}_d^0 H_{\text{eff}}^{\Delta B=2} B_d^0 \rangle_{\text{SUSY}}$
CAUX_H(109)	$D_{3,2}^{H^0}(\hat{s})$	CAUX_H(151)	$\langle \bar{B}_s^0 H_{\text{eff}}^{\Delta B=2} B_s^0 \rangle_{\text{SUSY}}$
CAUX_H(110)	$D_{3,3}^{H^0}(\hat{s})$
CAUX_H(111)	$D_{3,4}^{H^0}(\hat{s})$	CAUX_H(160)	$C_2^{(0)\text{SM}}(m_b^{\text{pole}})$
CAUX_H(112)	$D_{4,1}^{H^0}(\hat{s})$	CAUX_H(161)	$C_7^{(0)\text{SM}}(m_b^{\text{pole}})$
CAUX_H(113)	$D_{4,2}^{H^0}(\hat{s})$	CAUX_H(162)	$C_8^{(0)\text{SM}}(m_b^{\text{pole}})$
CAUX_H(114)	$D_{4,3}^{H^0}(\hat{s})$	CAUX_H(163)	$C_2^{(0)\text{SM}+H^\pm}(m_b^{\text{pole}})$
CAUX_H(115)	$D_{4,4}^{H^0}(\hat{s})$	CAUX_H(164)	$C_7^{(0)\text{SM}+H^\pm}(m_b^{\text{pole}})$
CAUX_H(116)	$D_{H^\pm, H^\pm}^{H^\pm}(\hat{s})$	CAUX_H(165)	$C_8^{(0)\text{SM}+H^\pm}(m_b^{\text{pole}})$
CAUX_H(117)	$D_{H^\pm, G^\pm}^{H^\pm}(\hat{s})$	CAUX_H(166)	$C_2^{(0)\text{SM}+H^\pm+\tilde{\chi}^\pm}(m_b^{\text{pole}})$
CAUX_H(118)	$D_{G^\pm, H^\pm}^{H^\pm}(\hat{s})$	CAUX_H(167)	$C_7^{(0)\text{SM}+H^\pm+\tilde{\chi}^\pm}(m_b^{\text{pole}})$
CAUX_H(119)	$D_{G^\pm, G^\pm}^{H^\pm}(\hat{s})$	CAUX_H(168)	$C_8^{(0)\text{SM}+H^\pm+\tilde{\chi}^\pm}(m_b^{\text{pole}})$
...	...	CAUX_H(169)	$C_S(m_b^{\text{pole}}) 1/\text{GeV}$
...	...	CAUX_H(170)	$C_P(m_b^{\text{pole}}) 1/\text{GeV}$
...	...	CAUX_H(171)	$C_{10}(m_b^{\text{pole}})$
...

Table 6: *The contents of the array CAUX_H, continued.*

CAUX_H(201)	λ_1
CAUX_H(202)	λ_2
CAUX_H(203)	λ_3
CAUX_H(204)	λ_4
CAUX_H(205)	λ_5
CAUX_H(206)	λ_6
CAUX_H(207)	λ_7
...
CAUX_H(211)	$\Delta_b \tan \beta / (1 + \Delta_b \tan \beta)$
CAUX_H(212)	$\Delta_t \cot \beta / (1 + \Delta_t \cot \beta)$
...
CAUX_H(221)	$S_{\text{SM}}^g(M_{H_1})$
CAUX_H(222)	$S_{\text{SM}}^g(M_{H_2})$
CAUX_H(223)	$S_{\text{SM}}^g(M_{H_3})$
...
CAUX_H(231)	$S_{\text{SM}}^\gamma(M_{H_1})$
CAUX_H(232)	$S_{\text{SM}}^\gamma(M_{H_2})$
CAUX_H(233)	$S_{\text{SM}}^\gamma(M_{H_3})$
...

Table 7: The updated contents of the array GAMBRN(IM, IWB=1, IH) for the decays of the neutral Higgs bosons H_{IH} . The entry GAMBRN(IM, IWB=1, IH) is for the decay width of the decay mode IM in GeV. And the entries GAMBRN(IM, IWB=2, IH) and GAMBRN(IM, IWB=3, IH) are the corresponding SM and the full SUSY branching ratios, respectively.

IM	Decay Mode	IM	Decay Mode	IM	Decay Mode
1	$H_{IH} \rightarrow e\bar{e}$	11	$H_{IH} \rightarrow ZZ$
2	$H_{IH} \rightarrow \mu\bar{\mu}$	12	$H_{IH} \rightarrow H_1Z$
3	$H_{IH} \rightarrow \tau\bar{\tau}$	13	$H_{IH} \rightarrow H_2Z$
4	$H_{IH} \rightarrow d\bar{d}$	14	$H_{IH} \rightarrow H_1H_1$
5	$H_{IH} \rightarrow s\bar{s}$	15	$H_{IH} \rightarrow H_1H_2$
6	$H_{IH} \rightarrow b\bar{b}$	16	$H_{IH} \rightarrow H_2H_2$
7	$H_{IH} \rightarrow u\bar{u}$	17	$H_{IH} \rightarrow \gamma\gamma$
8	$H_{IH} \rightarrow c\bar{c}$	18	$H_{IH} \rightarrow g g$
9	$H_{IH} \rightarrow t\bar{t}$	19	$H_{IH} \rightarrow Z\gamma$
10	$H_{IH} \rightarrow WW$	ISMN	GAMSM
IM	Decay Mode	IM	Decay Mode	IM	Decay Mode
ISMN+1	$H_{IH} \rightarrow \tilde{\chi}_1^0 \tilde{\chi}_1^0$	ISMN+11	$H_{IH} \rightarrow \tilde{\chi}_1^+ \tilde{\chi}_1^-$	ISMN+21	$H_{IH} \rightarrow \tilde{b}_2^* \tilde{b}_1$
ISMN+2	$H_{IH} \rightarrow \tilde{\chi}_1^0 \tilde{\chi}_2^0$	ISMN+12	$H_{IH} \rightarrow \tilde{\chi}_1^+ \tilde{\chi}_2^-$	ISMN+22	$H_{IH} \rightarrow \tilde{b}_2^* \tilde{b}_2$
ISMN+3	$H_{IH} \rightarrow \tilde{\chi}_1^0 \tilde{\chi}_3^0$	ISMN+13	$H_{IH} \rightarrow \tilde{\chi}_2^+ \tilde{\chi}_1^-$	ISMN+23	$H_{IH} \rightarrow \tilde{\tau}_1^* \tilde{\tau}_1$
ISMN+4	$H_{IH} \rightarrow \tilde{\chi}_1^0 \tilde{\chi}_4^0$	ISMN+14	$H_{IH} \rightarrow \tilde{\chi}_2^+ \tilde{\chi}_2^-$	ISMN+24	$H_{IH} \rightarrow \tilde{\tau}_1^* \tilde{\tau}_2$
ISMN+5	$H_{IH} \rightarrow \tilde{\chi}_2^0 \tilde{\chi}_2^0$	ISMN+15	$H_{IH} \rightarrow \tilde{t}_1^* \tilde{t}_1$	ISMN+25	$H_{IH} \rightarrow \tilde{\tau}_2^* \tilde{\tau}_1$
ISMN+6	$H_{IH} \rightarrow \tilde{\chi}_2^0 \tilde{\chi}_3^0$	ISMN+16	$H_{IH} \rightarrow \tilde{t}_1^* \tilde{t}_2$	ISMN+26	$H_{IH} \rightarrow \tilde{\tau}_2^* \tilde{\tau}_2$
ISMN+7	$H_{IH} \rightarrow \tilde{\chi}_2^0 \tilde{\chi}_4^0$	ISMN+17	$H_{IH} \rightarrow \tilde{t}_2^* \tilde{t}_1$	ISMN+27	$H_{IH} \rightarrow \tilde{\nu}_\tau^* \tilde{\nu}_\tau$
ISMN+8	$H_{IH} \rightarrow \tilde{\chi}_3^0 \tilde{\chi}_3^0$	ISMN+18	$H_{IH} \rightarrow \tilde{t}_2^* \tilde{t}_2$
ISMN+9	$H_{IH} \rightarrow \tilde{\chi}_3^0 \tilde{\chi}_4^0$	ISMN+19	$H_{IH} \rightarrow \tilde{b}_1^* \tilde{b}_1$	ISMN+ISUSYN	GAMSUSY
ISMN+10	$H_{IH} \rightarrow \tilde{\chi}_4^0 \tilde{\chi}_4^0$	ISMN+20	$H_{IH} \rightarrow \tilde{b}_1^* \tilde{b}_2$	ISMN+ISUSYN+1	GAMSM+GAMSUSY

References

- [1] J. S. Lee, M. Carena, J. Ellis, A. Pilaftsis and C. E. M. Wagner, “CPsuperH2.0: an Improved Computational Tool for Higgs Phenomenology in the MSSM with Explicit CP Violation,” *Comput. Phys. Commun.* **180** (2009) 312 [arXiv:0712.2360 [hep-ph]].
- [2] J. S. Lee, A. Pilaftsis, M. S. Carena, S. Y. Choi, M. Drees, J. R. Ellis and C. E. M. Wagner, “CPsuperH: A computational tool for Higgs phenomenology in the minimal supersymmetric standard model with explicit CP violation,” *Comput. Phys. Commun.* **156** (2004) 283 [arXiv:hep-ph/0307377].
- [3] M. Frank, T. Hahn, S. Heinemeyer, W. Hollik, H. Rzezhak and G. Weiglein, “The Higgs Boson Masses and Mixings of the Complex MSSM in the Feynman-Diagrammatic Approach,” *JHEP* **0702** (2007) 047 [hep-ph/0611326]; S. Heinemeyer, W. Hollik, H. Rzezhak and G. Weiglein, “The Higgs sector of the complex MSSM at two-loop order: QCD contributions,” *Phys. Lett. B* **652** (2007) 300 [arXiv:0705.0746 [hep-ph]]; T. Hahn, S. Heinemeyer, W. Hollik, H. Rzezhak and G. Weiglein, “FeynHiggs: A program for the calculation of MSSM Higgs-boson observables - Version 2.6.5,” *Comput. Phys. Commun.* **180** (2009) 1426.
- [4] G. Aad *et al.* [ATLAS Collaboration], “Observation of a new particle in the search for the Standard Model Higgs boson with the ATLAS detector at the LHC,” [arXiv:1207.7214 [hep-ex]]; S. Chatrchyan *et al.* [CMS Collaboration], “Observation of a new boson at a mass of 125 GeV with the CMS experiment at the LHC,” [arXiv:1207.7235 [hep-ex]].
- [5] S. Y. Choi, M. Drees and J. S. Lee, “Loop corrections to the neutral Higgs boson sector of the MSSM with explicit CP violation,” *Phys. Lett. B* **481** (2000) 57 [hep-ph/0002287].
- [6] S. Schael *et al.* [ALEPH and DELPHI and L3 and OPAL and LEP Working Group for Higgs Boson Searches Collaborations], “Search for neutral MSSM Higgs bosons at LEP,” *Eur. Phys. J. C* **47** (2006) 547 [hep-ex/0602042].
- [7] CMS Collaboration, “Search for Neutral Higgs Bosons Decaying to Tau Pairs in pp Collisions at $\sqrt{s}=7$ TeV,” CMS-PAS-HIG-11-029
- [8] J. Ellis, J. S. Lee and A. Pilaftsis, “Maximal Electric Dipole Moments of Nuclei with Enhanced Schiff Moments,” *JHEP* **1102** (2011) 045 [arXiv:1101.3529 [hep-ph]].
- [9] J. R. Ellis, J. S. Lee and A. Pilaftsis, “CERN LHC Signatures of Resonant CP Violation in a Minimal Supersymmetric Higgs Sector,” *Phys. Rev. D* **70** (2004) 075010 [hep-ph/0404167].
- [10] P. Z. Skands, B. C. Allanach, H. Baer, C. Balazs, G. Belanger, F. Boudjema, A. Djouadi and R. Godbole *et al.*, “SUSY Les Houches accord: Interfacing SUSY

spectrum calculators, decay packages, and event generators,” JHEP **0407** (2004) 036 [hep-ph/0311123].

- [11] B. C. Allanach, C. Balazs, G. Belanger, M. Bernhardt, F. Boudjema, D. Choudhury, K. Desch and U. Ellwanger *et al.*, “SUSY Les Houches Accord 2,” Comput. Phys. Commun. **180** (2009) 8 [arXiv:0801.0045 [hep-ph]].
- [12] M. S. Carena, J. R. Espinosa, M. Quiros and C. E. M. Wagner, “Analytical expressions for radiatively corrected Higgs masses and couplings in the MSSM,” Phys. Lett. B **355** (1995) 209 [hep-ph/9504316].
- [13] M. S. Carena, M. Quiros and C. E. M. Wagner, “Effective potential methods and the Higgs mass spectrum in the MSSM,” Nucl. Phys. B **461** (1996) 407 [hep-ph/9508343].
- [14] M. Carena, S. Gori, N. R. Shah and C. E. M. Wagner, “A 125 GeV SM-like Higgs in the MSSM and the $\gamma\gamma$ rate,” JHEP **1203** (2012) 014 [arXiv:1112.3336 [hep-ph]].
- [15] P. Bechtle, O. Brein, S. Heinemeyer, G. Weiglein and K. E. Williams, “HiggsBounds: Confronting Arbitrary Higgs Sectors with Exclusion Bounds from LEP and the Tevatron,” Comput. Phys. Commun. **181** (2010) 138 [arXiv:0811.4169 [hep-ph]].
- [16] M. Spira, “HIGLU: A program for the calculation of the total Higgs production cross-section at hadron colliders via gluon fusion including QCD corrections,” hep-ph/9510347.
- [17] R. V. Harlander and W. B. Kilgore, “Higgs boson production in bottom quark fusion at next-to-next-to leading order,” Phys. Rev. D **68** (2003) 013001 [hep-ph/0304035].
- [18] M. Ciccolini, A. Denner and S. Dittmaier, “Strong and electroweak corrections to the production of Higgs + 2jets via weak interactions at the LHC,” Phys. Rev. Lett. **99** (2007) 161803 [arXiv:0707.0381 [hep-ph]];
M. Ciccolini, A. Denner and S. Dittmaier, “Electroweak and QCD corrections to Higgs production via vector-boson fusion at the LHC,” Phys. Rev. D **77** (2008) 013002 [arXiv:0710.4749 [hep-ph]].
- [19] J. R. Ellis, J. S. Lee and A. Pilaftsis, “Electric Dipole Moments in the MSSM Reloaded,” JHEP **0810** (2008) 049 [arXiv:0808.1819 [hep-ph]].
- [20] M. Carena, J. R. Ellis, A. Pilaftsis and C. E. M. Wagner, “Renormalization-group-improved effective potential for the MSSM Higgs sector with explicit CP violation,” Nucl. Phys. B **586** (2000) 92 [arXiv:hep-ph/0003180].
- [21] A. Pilaftsis and C. E. M. Wagner, “Higgs bosons in the minimal supersymmetric standard model with explicit CP violation,” Nucl. Phys. B **553** (1999) 3 [hep-ph/9902371].
- [22] J. -J. Cao, Z. -X. Heng, J. M. Yang, Y. -M. Zhang and J. -Y. Zhu, “A SM-like Higgs near 125 GeV in low energy SUSY: a comparative study for MSSM and NMSSM,” JHEP **1203** (2012) 086 [arXiv:1202.5821 [hep-ph]];

M. Carena, S. Gori, N. R. Shah, C. E. M. Wagner and L. -T. Wang, “Light Stau Phenomenology and the Higgs $\gamma\gamma$ Rate,” JHEP **1207** (2012) 175 [arXiv:1205.5842 [hep-ph]];

K. Hagiwara, J. S. Lee and J. Nakamura, “Properties of 125 GeV Higgs boson in non-decoupling MSSM scenarios,” arXiv:1207.0802 [hep-ph];

G. F. Giudice, P. Paradisi and A. Strumia, “Correlation between the Higgs Decay Rate to Two Photons and the Muon $g - 2$,” arXiv:1207.6393 [hep-ph];

M. A. Ajaib, I. Gogoladze and Q. Shafi, “Higgs Boson Production and Decay: Effects from Light Third Generation and Vectorlike Matter,” arXiv:1207.7068 [hep-ph].

- [23] M. Carena, J. R. Ellis, A. Pilaftsis and C. E. M. Wagner, “Higgs-boson pole masses in the MSSM with explicit CP violation,” Nucl. Phys. B **625** (2002) 345 [arXiv:hep-ph/0111245].
- [24] J. R. Ellis, J. S. Lee and A. Pilaftsis, “B-Meson Observables in the Maximally CP-Violating MSSM with Minimal Flavour Violation,” Phys. Rev. D **76** (2007) 115011 [arXiv:0708.2079 [hep-ph]].
- [25] K. Cheung, O. C. W. Kong and J. S. Lee, “Electric and anomalous magnetic dipole moments of the muon in the MSSM,” JHEP **0906** (2009) 020 [arXiv:0904.4352 [hep-ph]].
- [26] J. Ellis, J. S. Lee and A. Pilaftsis, “A Geometric Approach to CP Violation: Applications to the MCPMFV SUSY Model,” JHEP **1010** (2010) 049 [arXiv:1006.3087 [hep-ph]].
- [27] A. Djouadi, V. Driesen, W. Hollik and A. Kraft, “The Higgs photon - Z boson coupling revisited,” Eur. Phys. J. C **1** (1998) 163 [hep-ph/9701342].
- [28] K. Cheung, T. -J. Hou, J. S. Lee and E. Senaha, “Higgs Mediated EDMs in the Next-to-MSSM: An Application to Electroweak Baryogenesis,” Phys. Rev. D **84** (2011) 015002 [arXiv:1102.5679 [hep-ph]].